ELSEVIER

Tectonophysics 305 (1999) 109–120

TECTONOPHYSICS

Mechanics of basin inversion

Mike Sandiford *

Department of Geology and Geophysics, University of Adelaide, South Australia, 5005, Adelaide, Australia

Received 1 March 1998; accepted 14 July 1998

Abstract

The long-term consequences of rifting for the thermal state of the deep crust and upper mantle reflect, in part, cooling induced by the reduction in heat production in the attenuated lithosphere and heating due to the burial of this heat production beneath the basin. Provided that the heat production is largely concentrated in the upper half of the crust, these factors result in significant increases in temperature at deep crustal and upper mantle levels. Because the Moho depth is likely to be reduced in the long-term limit of an isostatically balanced basin, these same factors may lead to slight cooling or slight heating of the Moho, depending on the nature of the basin-fill. For a Brace–Goetze lithospheric rheology (i.e. a rheology governed by a combination of frictional sliding and power-law creep), significant long-term lithospheric weakening (up to 5% per kilometre of basin-fill) accompanies basin formation when the lower crust is initially relatively strong and the basin fill is characterised by appreciable heat production and low thermal conductivity. In contrast, initially weak lower-crustal rheologies may result in long-term lithospheric strengthening. Evidence for basin-inversion in the geological record may therefore imply that heat production is strongly concentrated in the upper half of the crust and, under normal continental thermal regimes, the lower crust is strong.

Keywords: basin inversion; mechanics; lithosphere; extensional basins; rheology

1. Introduction

The inversion of sedimentary basins has received considerable interest in recent years, in part because of the important economic significance played by inverted structures in petroleum generation and trapping (see papers in Cooper and Williams, 1989, and Buchanan and Buchanan, 1995). To date most of this attention has focussed on the geometry and kinematics of inversion, with comparatively little attention devoted to questions of mechanics. One clear point of consensus to emerge from previous discussions of mechanics is that inversion represents the response to horizontal, in-plane, compressive stress fields, probably originating at the plate-scale (e.g. Hillis, 1995; Lowell, 1995). However, there is less consensus about the factors responsible for localisation of inversion within the basins as opposed to the surrounding hinterland. From the mechanical point of view, inversion in response to an in-plane, compressive stress field implies that the lithosphere on which the basin is developed remains sufficiently weak to localise regional contractional deformation long after the extensional basin forming episode. In particular, the interpretation that basin inversion occurs in response to in-plane compressive stress fields implies that the lithosphere on which the basin is developed is

* Tel.: +61 8 8303 35326; Fax: +61 8 8303 4347; E-mail: msandifo@geology.adelaide.edu.au

0040-1951/99/$ – see front matter
PII: S0040-1951(99)00023-2

weaker than surrounding lithosphere that did not witness earlier basin forming events. Previous discussions of mechanics have focussed on the role played by basin forming structures in localising subsequent contractional deformation (e.g. Sibson, 1995). However, such localisation may also reflect the fact that, in the first place, basin formation is determined by lithospheric strength variations that persist through basin formation. Alternatively, inversion may reflect fundamental changes in lithospheric strength as a direct consequence of basin formation itself. Recently, a number of workers have argued that basin formation is likely to result in long-term lithospheric strengthening (Ziegler et al., 1995; van Wees and Stephenson, 1995), although they may in some circumstances result in long-term lithospheric weakening (van Wees and Beekman, 1999). This paper explores the conditions for which basin formation may be an inherently weakening process, engendering the possibility that subsequent deformation will be localised beneath the previously formed basin.

Notions about the absolute strength of the lithosphere, the variation of strength with depth in the lithosphere, and the factors that control the strength of the lithosphere remain very rudimentary despite intense interest in recent years. This is mainly because the experimental basis of rheological models is necessarily carried out on laboratory scales and rates that are very different from those operating in nature. Of particular concern is the temperature dependence of lithospheric rheology. Many contemporary models for lithospheric strength employ rheologies that are extremely temperature-sensitive (eg. Brace and Kohlstedt, 1980; Kohlstedt et al., 1995). This is certainly the case for the rheological models based on a combination of frictional sliding and various creep mechanisms. These models, which we term the Brace–Goetze model (Molnar, 1989), have become something of a *de facto* standard for numerical models of lithospheric deformation (eg. Brace and Kohlstedt, 1980; Sonder and England, 1986; Ord and Hobbs, 1989; Kohlstedt et al., 1995). Neil and Houseman (1997) have shown that, for a lithosphere whose rheology is controlled by power-law creep, spatial variations of Moho temperature of only $\sim$20ºC may account for the observed partitioning of deformation in continental interiors such as Central Asia. With such sensitivity, processes that subtly change the thermal regime of the lithosphere (such as basin formation) might be expected to impact on rates and distribution of subsequent deformation! Clearly, one of the paramount challenges in lithospheric geodynamics is to find geological observations pertinent to testing models of lithospheric rheology.

With these views in mind, this paper focuses on the impact of basin formation on the integrated strength of the Brace–Goetze lithosphere. The intention is to elaborate the long-term, deep-level, thermal response to basin development and its implications for long-term changes in lithospheric strength. The focus is on basins developed as a consequence of lithospheric stretching in cratonic settings. In such settings, it may be readily appreciated that the elevated thermal regimes attendant with rifting may lead to short-term reductions in lithospheric strength (although this need not necessarily be the case as shown by England, 1983). However, the geological record shows that basin inversion may occur many 10's to 100's of millions of years after the initial stretching events leading to the basin formation (see papers in Cooper and Williams, 1989, and Buchanan and Buchanan, 1995). The objective of this paper is to examine the role played by the crustal heat production distribution on the long-term thermal and mechanical response to basin formation, following thermal subsidence. In a companion paper (Hand and Sandiford, 1999) the results of the analysis presented in this paper are applied to the development of intracratonic orogeny associated with basin inversion in central Australia.

2. Thermal considerations

The focus of this study is the long-term consequences of sedimentary basin development on the mechanical state of the lithosphere. Basin development is often a consequence of lithospheric strain (such as extensional deformation), which alters the compositional and thermal structure of the lithosphere. Therefore, the comparison of lithospheric strength immediately prior to and well after basin formation requires evaluation of the basin forming mechanism. In rift basins, formed in response to extensional strain (Fig. 1) as elaborated by McKen-

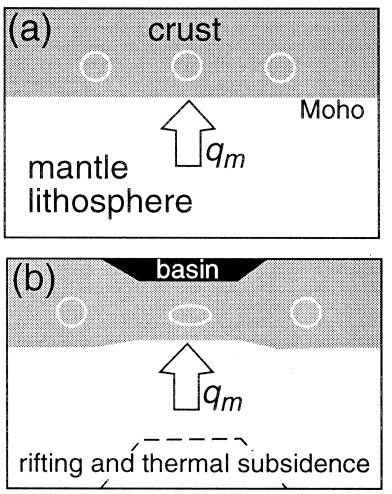

Fig. 1. Illustration of the basin forming mechanism modelled in this paper (see text for discussion): (a) initial lithosphere priori to basin formation; (b) lithosphere after rifting and thermal subsidence.

zie (1978), subsidence results from both the initial stretching of the lithosphere (the rift phase) as well as its subsequent cooling (the thermal subsidence phase). In this paper, I evaluate the long-term mechanical consequences of basin formation by contrasting the thermal structure and mechanical strength of the pre-rift lithosphere with that of the extended lithosphere following thermal re-equilibration; that is after both rift and thermal subsidence. The scenario described here is therefore appropriate to basin inversion events occurring more than 50–100 m.y. after initial rifting. For inversion events occurring less than 50 m.y. after the initial rifting events, additional thermal transients associated with the rifting are likely to play an important role in controlling strength distributions in the lithosphere.

As noted above, and elaborated in further detail in the next section, estimates of the strength of the Brace–Goetze lithosphere are sensitive to the thermal structure of the lithosphere, and particularly the temperature of the upper mantle (e.g. Sonder and England, 1986; Molnar, 1989). Therefore, a qualitative understanding of the impact of basin formation can be obtained by evaluating the long-term temperature changes at depths appropriate to the uppermost mantle depths ($\Delta T_{z\sim 35\ \mathrm{km}}$ — see Table 1 for definition of symbols). The strength of the lithosphere is also likely to be sensitive to the temperature at strength-controlling, compositional boundaries within the lithosphere, such as the Moho. Since the depth to such boundaries is likely to change as a consequence of basin formation, the temperature changes they experience will be different from ΔT_z. An analysis of the thermal consequences of rift-basin development in terms of both $\Delta T_{z=35\ \mathrm{km}}$ and ΔT_{Moho} is presented below.

The long-term thermal evolution of rift basins is a consequence of the deformation-induced imbalance between heat loss through the attenuated lithosphere and the heat supplied to the base of the lithosphere (McKenzie, 1978). The post-rift evolution (the so-called thermal subsidence) reflects lithospheric cooling, which restores this balance. The following sections provide estimates of both $\Delta T_{z=35\ \mathrm{km}}$ and ΔT_{Moho} following the return to this balance (that is, after the pre-rift basal heat flow q_{m} is re-established). This strategy differs from previous studies based on the assumption cooling acts to restore the pre-rift lithospheric thickness (e.g., van Wees and Stephenson, 1995), and reflects the fact that thermal subsidence is primarily a problem in thermal conduction. The reference-state against which changes in temperature are measured is provided by the steady-state thermal regime in the pre-rift lithosphere.

A simple distribution of heat production in the initial (pre-rift) lithosphere is modelled, in which all heat production is confined to a layer extending from the surface to depth h_{r}. The heat production H_{c} in this layer is assumed to be uniform (Fig. 2a). I make the 1-D approximation appropriate to wide basins developed above a laterally uniform lithosphere in which all heat flow is in the vertical direction. Attenuation of the heat-producing layer during rifting necessarily reduces the thickness of this layer by the stretching factor β (Fig. 2b). While the reduction in the thickness of the heat-producing layer should be expected to cause long-term cooling, this will be countered to some extent by heating due to the burial of the remaining heat production beneath the basin (Fig. 2a,b). As shown in Fig. 3, the relative magnitude of the cooling induced by the attenuation of heat production and the heating induced by its burial is sensitive to the total amount of heat production as well as its distribution in the lithosphere and the amount of stretching associated with basin

Table 1
Default thermal parameter ranges for initial (pre-rift) lithosphere and basin-filling sediment (default normalised values are between brackets)

Symbol	Parameter	Normalisation/equivalence	Default value
ΔT_z	temperature change experienced at depth z	$\Delta T(1)+\Delta T(2)+\Delta T(3)$	
ΔT_{Moho}	temperature change experienced by the Moho	$\Delta T(1)+\Delta T(2)+\Delta T(3)+\Delta T(4)$	
$\Delta T(1)$	temperature change at depth z due to attenuation of pre-existing crustal heat production		
$\Delta T(2)$	temperature change at depth z due to heat production in the basin-fill		
$\Delta T(3)$	temperature change at depth z due to conductivity contrast between basin-fill and pre-existing crust		
$\Delta T(4)$	temperature change experienced by the Moho due to a change in depth.		
q_c	crustal contribution to heat flow		30 mW m^{-2}
q_m	mantle heat flow	$q'_m = q_m/q_c$	30 mW m^{-2} (1.0)
h_r	length-scale for heat production	$h'_r = h_r/z_c$	11.7 km (0.33)
z_c	crustal thickness		35 km
H_c	upper crustal heat production	q_c/h_r	2.6 μW m^{-3}
H_s	basin-fill heat production	$H'_s = H_s h_r/q_c$	1.3 μW m^{-3} (0.5)
k_c	crustal conductivity		3 W m^{-1} K^{-1}
k_s	basin-fill conductivity	$k'_s = k_s/k_c$	3 W m^{-1} K^{-1} (1.0)
ρ_m	density of lithospheric mantle		3350 kg m^{-3}
ρ_c	density of crust		2750 kg m^{-3}
ρ_s	density of basin-fill	$\rho'_s = (\rho_c - \rho_s)/(\rho_m - \rho_c)$	2350 kg m^{-3} (0.66)
β	stretching factor associated with initial basin formation		

formation. Additional factors that influence the thermal regime in the deeper lithosphere beneath a basin include: (1) the heat production within the basin-filling sediments, which adds to the heat production contributed by the attenuated lithospheric column (Fig. 4a), and (2) differences in the thermal conductivity of the basin-fill and the underlying crust which may change near-surface temperature gradients (Fig. 4b).

In addition to admitting concise analysis, the heat production distribution outlined above and illustrated in Fig. 2 concords with the prevailing prejudice that heat production is strongly concentrated in the upper parts of the lithosphere (e.g. Lachenbruch, 1968). While the precise details of natural heat production distributions are debatable, the distribution used here preserves the first-order features of any distribution that is restricted to the upper parts of the lithosphere.

The extent of rifting can be characterised by either the stretching factor β or the thickness of the basin-fill z_s developed in response to both rifting and thermal subsidence in the long-term limit of a locally compensated, sediment-filled basin. The stretching factor is related to the thickness of the basin-fill by:

$$\beta \approx \frac{z_c}{z_c - z_s(1+\rho')}$$

where z_c is the initial thickness of the crust, and ρ' is a normalised density given by:

$$\rho' = \frac{\langle \rho_c \rangle - \langle \rho_s \rangle}{\langle \rho_m \rangle - \langle \rho_c \rangle}$$

where ρ_s, ρ_c and ρ_m are the densities of the basin-fill, crust and lithospheric mantle, respectively, and the angle brackets specify the mean taken over the appropriate layer.

Prior to rifting the contribution of the lithospheric heat production to the initial surface heat flow is $q_c = H_c h_r$ (Fig. 2a), with the initial surface heat flow $q_s = q_c + q_m$. Following rifting, the contribution of these pre-existing lithospheric sources to surface heat flow is q_c/β (Fig. 2b). The long-term change in temperature due to attenuation of the pre-existing heat production and its burial beneath the basin is given by (see Fig. 2):

$$\Delta T(1)_{z>z_s+h_r/\beta} \approx \frac{H_c h_r \left(h_r + 2z_s\beta - h_r\beta^2\right)}{2\langle k_c \rangle \beta^2}$$

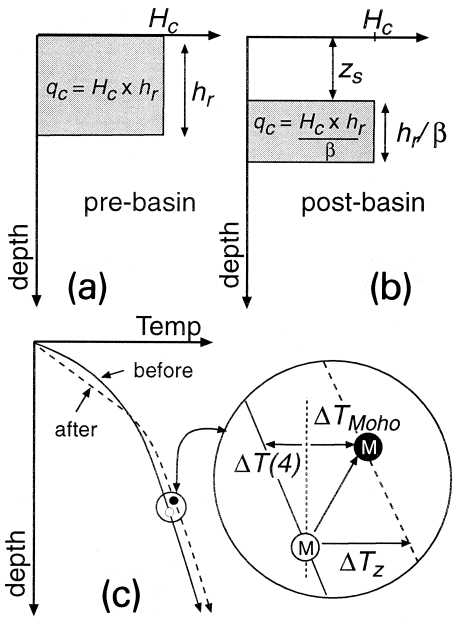

Fig. 2. (a) Modelled heat production prior to basin development, characterised by an upper crustal layer of thickness h_r producing heat at rate H_c. (b) Heat production distribution following basin stretching (by factor β) sufficient to generate basin-fill of thickness z_s. (c) Schematic geotherms before (solid line), and after (dashed line), rifting and associated thermal subsidence. The changes in the heat production distribution lead to changes in temperature at a given depth (ΔT_z — see inset). The Moho temperature changes (ΔT_{Moho}) differ from ΔT_z because Moho depths (as represented by small circles) are likely to be reduced in the long-term limit of an isostatically balanced rift-basin (see text for discussion). $\Delta T(4)$ provides a measure of the cooling due to the change in depth of the Moho, with $\Delta T_{Moho} = \Delta T_z + \Delta T(4)$ (see text for discussion).

where $\langle k_c \rangle$ is the mean thermal conductivity of the crust. Note that this relation applies only at levels below that containing heat production, i.e. $z > z_s + h_r/\beta$. Fig. 3c shows ΔT_z due to attenuation and burial of the pre-existing heat production for a variety of different heat production distributions, using default thermal parameters as listed in Table 1. Note that increasing the thickness of the heat-producing layer, while keeping the total amount of heat produced by the layer constant, causes significant reductions in ΔT_z (cf. Fig. 3c,d).

Clastic sediments typically contain significant concentrations of heat-producing elements and the additional heat production contributed by the basin-fill (typically 1–3 $\mu W\ m^{-3}$) will cause some heating of

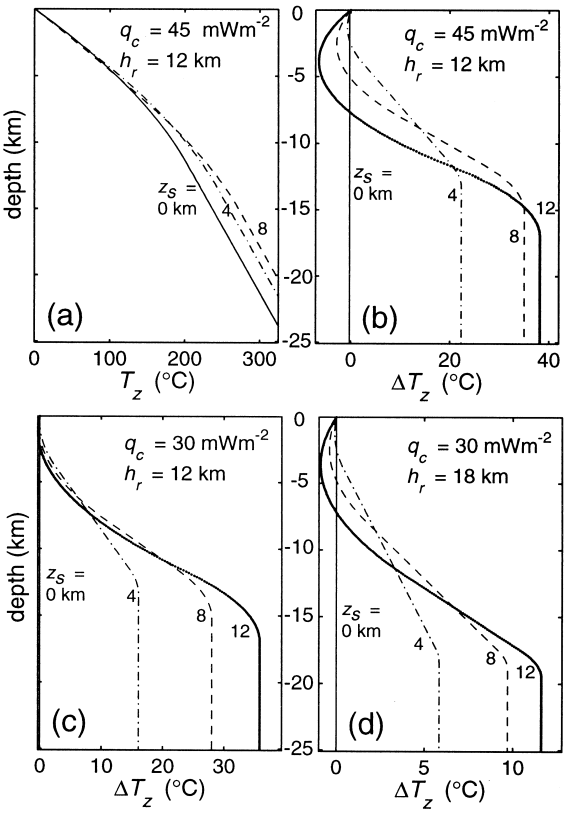

Fig. 3. (a) Geotherms and (b, c and d) ΔT_z as a function of depth for various values of basin-fill ($z_s = 0$, 4, 8 and 12 km). Default parameters values are as listed in Table 1 with exceptions noted on the individual figures.

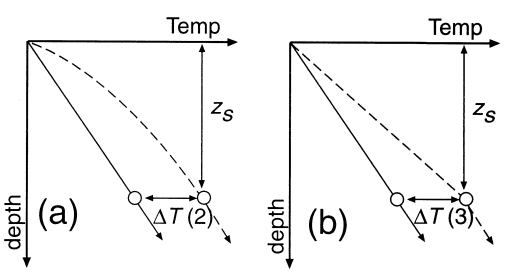

Fig. 4. (a) the effect of basin-fill heat production on the thermal regime of the upper crust ($\Delta T(2)$). (b) The effect of conductivity contrasts between the basin-fill and the underlying crust ($\Delta T(3)$). The solid line illustrates schematic geotherms with (a) no heat production in the basin-fill and (b) no thermal conductivity contrast across the basin-fill and the underlying crust. The dashed lines indicate the general form of geotherms expected by (a) introducing significant heat production in the sediment, and (b) lowering the mean conductivity of the basin-fill relative to the underlying crust.

the underlying lithosphere (Fig. 4a). Assuming that the distribution of heat production is homogeneously distributed in the basin-fill, then the change in temperature due to this heat production, $\Delta T(2)$, at any depth beneath the base of the sequence, $z > z_s$, is:

$$\Delta T(2)_{z>z_s} \approx \frac{\langle H_s \rangle z_s^2}{2\langle k_s \rangle}$$

where $\langle H_s \rangle$ and $\langle k_s \rangle$ represent the mean heat production and thermal conductivity of the basin-fill.

Because the thermal conductivity of the basin-fill maybe different from that in crystalline rocks that comprise cratonic crust, the basin may provide an insulating effect causing changes in the temperatures in the underlying crust (Fig. 4b). The effect of a conductivity contrast between the basin-fill and the underlying crust, $\Delta T(3)$ can be approximated as:

$$\Delta T(3)_{z>z_s} \approx z_s q_s \left(\frac{1}{\langle k_s \rangle} - \frac{1}{\langle k_c \rangle} \right)$$

where q_s $(= q_m + q_c/\beta)$ is the heat flow at the base of the sedimentary pile.

The temperature change at any depth greater than the base of the heat-producing layer due to rift basin development is thus:

$$\Delta T_{z>z_s+h_r/\beta} \approx \Delta T(1) + \Delta T(2) + \Delta T(3)$$

In order to track the long-term change in depth to the Moho following rifting and subsidence I assume local isostatic compensation as appropriate to wide basins. In this case the displacement of the Moho is dependent on the relative densities of the basin fill, the crust and the mantle. The corresponding change in temperature of the Moho due to the change in depth is dependent on the steady-state temperature gradient in the deep crust (ie., $q_m/\langle k_c \rangle$):

$$\Delta T(4) \approx \frac{z_s q_m \rho'}{\langle k_c \rangle}$$

The total long-term change in Moho temperature due to rift basin formation is therefore:

$$\Delta T_{Moho} \approx \Delta T(1) + \Delta T(2) + \Delta T(3) + \Delta T(4)$$

Note that in the typical scenario where $\langle \rho_c \rangle > \langle \rho_s \rangle$, the Moho shallows as the long-term consequence of basin formation. Consequently, $\Delta T(4)$ will be negative and $\Delta T_{Moho} < \Delta T_{z=35\ km}$.

Default parameter values for the reference lithosphere (see Table 1) are used to illustrate the thermal response of a typical continental lithosphere. This lithosphere is characterised by a initial surface heat flow of 60 mW m^{-2}, of which half is due to sources in the upper third of the crust (q_c = mW m^{-2}) and half due to mantle heat flow (q_m = mW m^{-2}). For the basin-fill, the following default parameters are used: heat production equal to 50% of the upper crustal heat production value ($H_s = 0.5\ q_c/h_r$), thermal conductivity equal to that of the basement ($k_s = k_c$), and density equal to 2350 km^{-3} giving a value of ρ' of 0.66. Figs. 5 and 6 show the predicted changes in $\Delta T_{z=35\ km}$ and ΔT_{Moho} as a function of basin thickness for the default parameter values (dashed lines) as well as plausible range about the default values (solid lines). In Figs. 5 and 6 values of default parameter values are shown normalised against relevant crustal parameters.

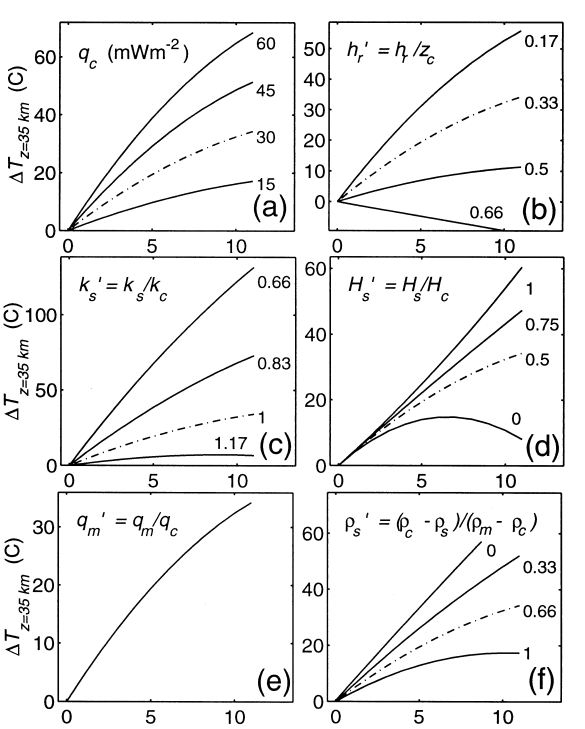

Fig. 5. Illustration of the long-term changes in $\Delta T_{z=35\ km}$ as a function of basin formation for plausible ranges in the various thermal parameters. Default parameter values as listed in Table 1 are indicated by dashed lines, with plausible ranges in the various parameters indicated by the solid lines (see text for discussion).

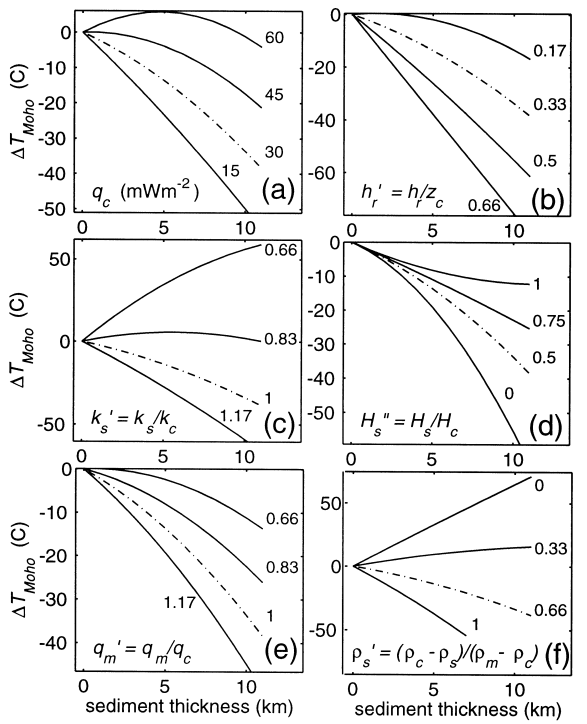

Fig. 6. Illustration of the long-term changes in ΔT_{Moho} as a function of basin formation for plausible ranges in the various thermal parameters. Default parameter values as listed in Table 1 are indicated by dashed lines, with plausible ranges in the various parameters indicated by the solid lines (see text for discussion).

Figs. 5 and 6 illustrate that for the default parameter value, $\Delta T_{z=35\ \mathrm{km}}$ is estimated to be positive ($\sim$3ºC per km of basin-fill), implying heating at any given depth, while ΔT_{Moho} is negative (~ -3ºC per km of basin-fill), implying Moho cooling. These subtle changes are sensitive to plausible variations in the parameter values, as illustrated in Figs. 5 and 6 and outlined below.

(1) *Total basement heat production*, q_{c} (Fig. 5a, Fig. 6a): changes in the contribution of the basement heat production changes the magnitude of $\Delta T_{z=35\ \mathrm{km}}$ in linear proportion to q_{c}. For plausible values of q_{c}, ΔT_{Moho} remains negative, although for values of $q_{\mathrm{c}} > 45$ mW m^{-2}, the predicted reductions in Moho temperature are negligible.

(2) *Length-scale for basement heat production*, h_{r} (Fig. 5b, Fig. 6b): for a given value of q_{c}, increasing the characteristic length-scale of the basement heat production distribution reduces the temperature rises associated with basin formation, reflecting the fact that the magnitude of the cooling effect due to attenuation of basement heat production relative to the heating due to its burial is a sensitive function of h_{r}. For $h_{\mathrm{r}}' > 0.5$ ($h_{\mathrm{r}} > 17.5$ km), basin formation results in cooling of the deep crust and upper mantle (i.e. $\Delta T_{z=35\ \mathrm{km}} < 0$),

(3) *Basin thermal conductivity* (Fig. 5c, Fig. 6c): introducing thermal conductivity contrasts across the basement–basin interface can result in profound temperature changes in the deeper lithosphere. For example, a reduction in basin-fill thermal conductivity relative to the basement by $\sim$33% results in increase in $\Delta T_{z=35\ \mathrm{km}}$ (and ΔT_{Moho}) of a $\sim$10ºC per kilometre of basin-fill.

(4) *Basin heat production*, H_{s} (Fig. 5d, Fig. 6d): the magnitude of the heat production in the basin-fill provides an important control on the deep thermal structure, contributing to $\Delta T_{z=35\ \mathrm{km}}$ by up to 4ºC per μW m^{-3} of heat production in the basinal sediments at $z_{\mathrm{s}} = 5$ km and 16ºC per μW m^{-3} at $z_{\mathrm{s}} = 10$ km.

(5) *Long-term mantle heat flow*, q_{m} (Fig. 5e, Fig. 6e): since $\Delta T_{z=35\ \mathrm{km}}$ is simply dependent on changes in the thermal configuration of the crust (i.e. $\Delta T(1)$, $\Delta T(2)$ and $\Delta T(3)$), it is unaffected by the magnitude of mantle heat flow and consequently there is only one curve in Fig. 5e. However, the value of q_{m} profoundly affects the estimated value of ΔT_{Moho}, with lower q_{m} favouring higher ΔT_{Moho}. A decrease in q_{m} of 10 mW m^{-2} results in an increase in the estimated value of $\sim$2ºC for each additional kilometre of basin-fill.

(6) *Density of the basin fill*, ρ_{s} (Fig. 5f, Fig. 6f): the density of the basin-fill affects the amount of stretching needed to generate a given basin thickness, as well as the depth to the Moho in the long-term limit of an isostatically balanced lithospheric column. For $\rho_{\mathrm{s}} = \rho_{\mathrm{c}}$ (i.e., $\rho' = 0$), there is no long-term shallowing of the depth to the Moho and consequently $\Delta T_{\mathrm{Moho}} = \Delta T_{z=35\ \mathrm{km}}$. In general, an increase in ρ_{s} will lead to an increase in ΔT_{Moho} because the terminal Moho depth is deeper.

The results listed above show that both the magnitude and the sign of the $\Delta T_{z=35\ \mathrm{km}}$ and ΔT_{Moho} are sensitive functions of the thermal character of both the pre-rift crust and the basin-fill. From the mechanical point of view an important result is that while basin formation may lead to slight, long-term

cooling of the Moho, it will generally lead to long-term increases in the temperature at any given depth in the upper mantle.

3. Mechanical considerations

In many instances basin inversion appears to involve whole lithospheric deformation (e.g. Hillis, 1995), and thus the mechanics of basin inversion must be evaluated in light of appropriate models of lithospheric rheology. Lithospheric rheology is generally thought to be temperature-dependent and particularly sensitive to the thermal state of the upper mantle (e.g. Sonder and England, 1986; England, 1987). A popular, generalised model for lithospheric rheology which incorporates a temperature sensitivity is the so-called Brace–Goetze model (see Molnar, 1989). In this model the lithosphere is assumed to deform by a combination of frictional sliding and power-law creep mechanisms (see Table 2 for parameter ranges used in calculations; Fig. 7). To evaluate the consequences of basin formation for the Brace–Goetze lithosphere we assume a compositional stratification with different rheological parameters for the basin-fill, the pre-existing crust and the mantle (the rheological parameters used for the various flow laws are listed in Table 1). The rheological parameters for

Table 2
Flow parameters for power law creep

Parameter	1	2	3	4	5
Power-law exponent	1.9	3.1	4.2	3.4	3.6
Pre-exponential constant	0.001995	0.07943	12589	10000	31623
Activation energy	141	243	445	498	535

Columns: (1) basin-fill (modelled on Westerly granite); (2) weak crust (modelled on Adirondack granulite); (3) strong crust (modelled on Pikwitonei granulite); (4) weak mantle (modelled on Anita Bay dunite); (5) strong mantle (modelled on dry dunite). Data taken from Liu and Zoback (1997).

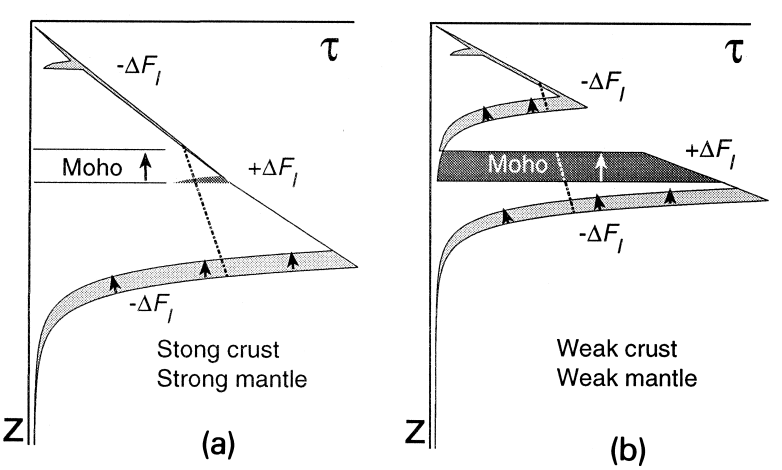

Fig. 7. Schematic illustration of the long-term strength changes in a Brace–Goetze lithosphere following basin formation. The strength of the lithosphere is proportional to the area under the τ–z curve. Relative changes in strength are primarily due to: (1) changes in the thermal structure, which generally leads to decreases in strength (as indicated by light shade); and (2) a reduction in the depth to the Moho, which increases the strength (as indicated by dark shade). Lithosphere characterised by relatively strong crust will be dominated by the former and hence show long-term strength reductions (a), whereas lithosphere characterised by weak lower crust may show long-term strength increases (b). The dashed lines serve to illustrate that this qualitative behaviour is preserved for more refined rheological models that include additional strength limiting flow-laws, specifically flow-laws that occlude the large stress magnitudes characterising the frictional sliding to temperature-dependent creep transition in the Brace–Goetze model (e.g. Kohlstedt et al., 1995).

rock types that could arguably represent the various parts of the crust–mantle system show considerable variation and consequently any particular rheological model is subject to considerable uncertainty (see further discussion below). In the calculations presented below, the role of variable strength crust and mantle is investigated by using creep parameters that span a range from relatively weak to relatively strong. I have used creep parameters (see Table 2) appropriate to Pikwitonnei granulite (weak crust), Adirondack granulite (strong crust), Anita Bay dunite (weak mantle) and dry dunite (strong mantle).

Before discussing the results of numerical calculations performed using the Brace–Goetze model, it is worth summarising some of the limitations of this kind of modelling. Most importantly, the uncertainty in the material constants governing flow of rocks implies very large uncertainties in the strength of the lithosphere, as described by Molnar (1989). Similarly, uncertainties in the thermal structure of lithosphere lead to large uncertainties in calculated strength. For example, an uncertainty in the Moho temperature of 100ºC produces a factor of 2 error in calculated strength at a given strain rate or an order of magnitude error in strain rate at a given strength (e.g., Molnar, 1989). In comparison, estimates of the relative change in strength accompanying changes in other environmental variables, such as temperature, are likely to be far more robust. In the discussion below we concentrate on relative changes in strength accompanying the long-term thermal changes associated with rift basin development.

In the calculations presented below, the strength of the lithosphere F_l is defined as the vertical integral of the shear stress (Fig. 7), with the shear stress defined at a strain rate of 10^{-16} s^{-1}. The thermal state of the lithosphere is governed by 1-D steady-state conduction, an approximation appropriate to wide basins. For narrower basins where the width is less than a few times the thickness of the lithosphere, the dissipating effects of lateral heat conduction will diminish the thermal impact of basin formation and correspondingly diminish the mechanical consequences. Because we are interested in relative changes in strengths, rather than absolute strengths, all strengths are normalised against the strength of the initial or pre-rift lithosphere ($\Delta F_l = F_l(z_s)/F_l(z_s = 0)$).

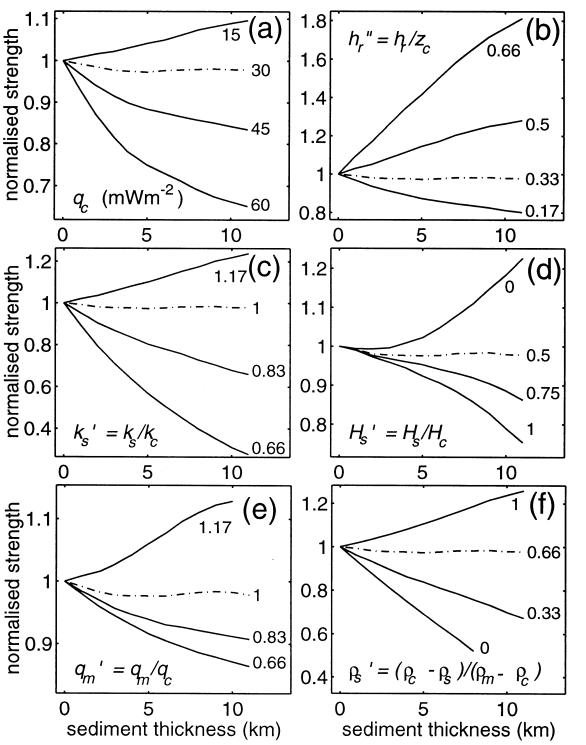

Fig. 8. Illustration of the long-term changes in lithospheric strength as a function of basin formation for plausible ranges in the various thermal parameters. Default thermal parameter values as listed in Table 1 are indicated by dashed lines, with plausible ranges in the various parameters indicated by the solid lines (see text for discussion). Strength parameters appropriate to a weak crust–weak mantle configuration as listed in Table 2.

The long-term strength changes (ΔF_l) accompanying rift basin formation are shown for a weak crust–weak mantle configuration in Fig. 8 and for a strong crust–strong mantle configuration in Fig. 9. For the default thermal parameter range, the weak lithospheric configuration shows virtually no long-term change in lithospheric strength, while the strong lithospheric configuration shows weakening by about 1% per kilometre of basin fill. In both cases, lower thermal conductivities and/or higher heat production and density in the basin fill, may potentially induce significant weakening, while an increase in the characteristic length-scale for heat production leads potentially to dramatic strengthening.

The different response to basin formation for the different rheological configurations reflects the

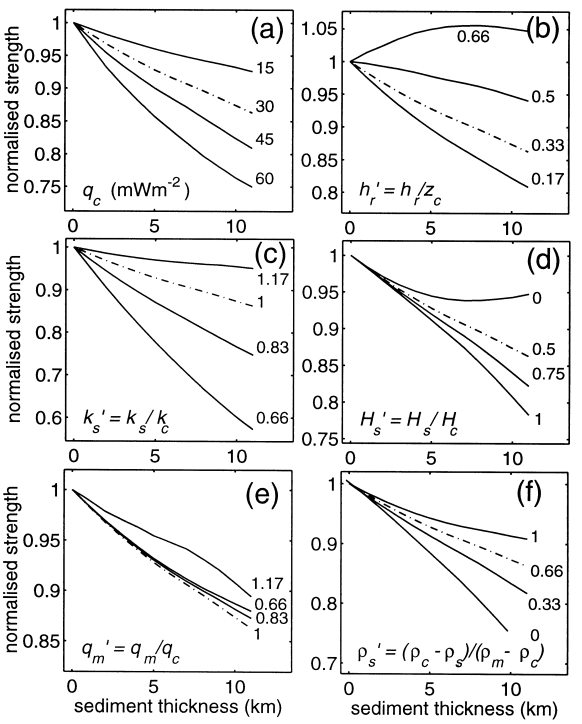

Fig. 9. As for Fig. 8 but with strength parameters appropriate to strong crust–strong mantle configuration (see Table 2).

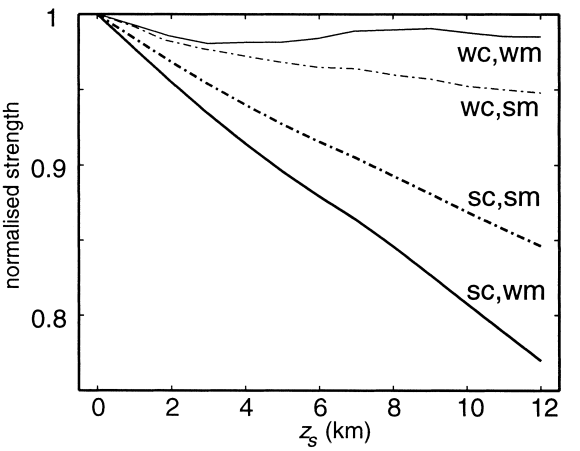

Fig. 10. Comparison of the effect of various combinations of creep parameters on the strength for default thermal parameter values. Abbreviations are as follows: *wm* = weak crust; *sc* = strong crust; *wm* = weak mantle; *sm* = strong mantle (see text for discussion).

relative weighting of two of the factors contributing to strength changes (Fig. 7). The first, due to the changes in the temperature structure of the upper mantle, generally induces lithospheric weakening. The second, due to the shallowing of the Moho, leads to a significant strengthening only in the case when the lower crust of the pre-rift lithosphere is relatively weak (Fig. 7). Other factors that affect the strength changes of the Brace–Goetze lithosphere include the temperature structure in the mid-deep crust, which may affect the creep-strength of the crust, and the creep strength of the basin. Fig. 10 shows that for the default thermal parameter range, the creep strength of the crust is critical to the strength changes during basin formation, with the creep strength of the upper mantle providing a second-order effect.

While Figs. 8 and 9 illustrate the role of the individual thermal parameters on ΔF_l, it is not so clear how plausible combinations of thermal parameters (especially for the basin-fill) may affect the magnitude (and sign) of ΔF_l. In order to illustrate this, Fig. 11 shows two idealised basins-fills, modelled on a carbonate-dominated fill (Model A with relatively high thermal conductivity and density and low heat production) and a shale-dominated fill (Model B with low thermal conductivity and density and high heat production). Parameter ranges for these model basin-fills are listed in Table 3, and calculated ΔF_l, ΔT_{Moho} and $\Delta T_{z=35\ km}$ shown in Fig. 11. Model B results in very high $\Delta T_{z=35\ km}$ which leads to dramatic weakening for all rheological configurations, with the most dramatic weakening produced by the weak-mantle configurations. As may be expected, Model A shows much lower strength changes than Model B, implying that the nature of the basin-fill can exert a profound influence on the subsequent inversion-potential of any given basin.

4. Discussion

The calculations summarised in the previous sections illustrate that the long-term thermal and mechanical response of the lithosphere to rift basin formation is sensitive to (1) the distribution of the heat sources in the pre-rift lithosphere, (2) the relative strength of lower-crust and upper mantle in the pre-rift lithosphere, and (3) the thermal character and density of the basin-fill. Long-term lithospheric weakening is favoured by heat production distri-

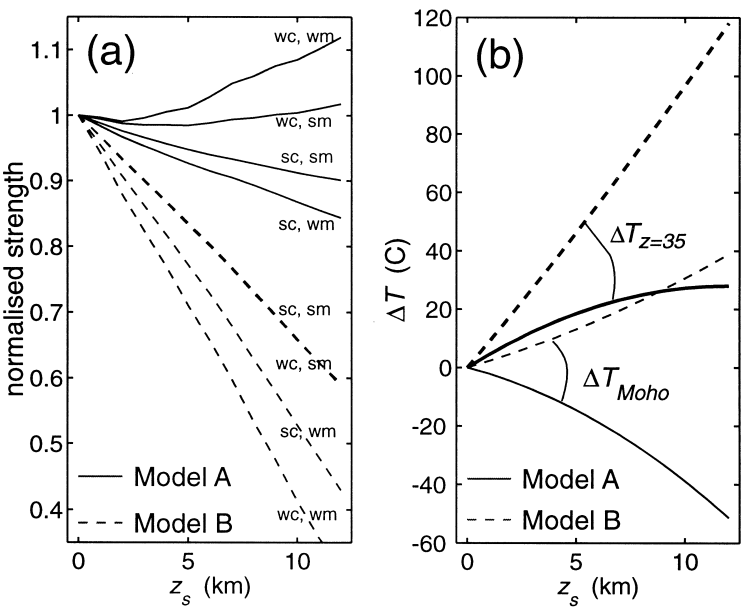

Fig. 11. Illustration of the long-term changes in lithospheric strength (a) and $\Delta T_{z=35\ \mathrm{km}}$ and ΔT_{Moho} (b) for a carbonate-dominated basin (Model A: solid lines) and a shale-dominated basin (Model B: dashed lines) with model parameters as listed in Table 3 (other values are the defaults as listed in Table 1). (a) All four combinations of weak and strong crust and mantle flow parameters, for each model, as listed in Table 2, with solutions appropriate to a strong crust indicated by the thick lines. Abbreviations are as follows: *wm* = weak crust; *sc* = strong crust; *wm* = weak mantle; *sm* = strong mantle (see text for discussion).

butions strongly concentrated in the upper 1/2 of the crust, relatively strong lower crust in the pre-rift lithosphere, and basin-fill characterised by low thermal conductivity and high heat production and density. With appropriate combinations within the plausible ranges for the relevant parameters, the estimated weakening can be as much as 5% per kilometre of basin-fill. In particular, basins with a fill dominated by shale can show dramatic weakening due to the high heat production and low thermal conductivity associated with the fill.

Table 3
Parameter ranges for model basin-fill

Model	Symbol	Value
Model A	H_s	0.5 μW m^{-3}
	k'	1.0
	ρ_s	2600 kg m^{-3}
	ρ'	0.25
Model B	H_s	2.5 μW m^{-3}
	k'	0.85
	ρ_s	2300 kg m^{-3}
	ρ'	0.75

Model 1 is based on a notional carbonate-rich basin (i.e. relatively high thermal conductivities and densities and low heat production rates), while Model 2 is based on a notional shale-dominated basin (i.e. high heat-production rates and low thermal conductivities and densities).

The estimated magnitude of the weakening provides a plausible physical basis for the common occurrence of inverted structures formed long after basin development (see papers in Cooper and Williams, 1989, and Buchanan and Buchanan, 1995). Indeed, the calculations presented here suggest that such basin inversion may provide an independent constraint on the thermal and mechanical structure of the lithosphere. While the notion that heat production is strongly concentrated in the upper parts of the crust is well entrenched (e.g. Lachenbruch, 1968), constraints on the relative strengths of the lower crust and upper mantle under normal continental thermal regimes are less well understood. The results of the analysis presented here suggest

that basin-inversion may have the potential to provide new insights into this problem. The rheological model used in the calculations summarised in this paper is necessarily approximate. In particular, there is considerable doubt about the factors controlling strength near the transition from frictional sliding to thermally activated creep. Many workers have argued that the Brace–Goetze model may significantly overestimate the strength at this transition (e.g. Kohlstedt et al., 1995). While modifications to the Brace–Goetze model are likely to affect the absolute magnitude of the calculated strength changes, it is unlikely that the qualitative features of the calculations outlined will be affected. As illustrated in Fig. 7, it is probable that the different behaviour of the strong and weak lower crustal configurations (Figs. 10 and 11) will be robust to changes in the absolute magnitude of the strength at the transition from temperature-independent to temperature-dependent deformation mechanisms (see Fig. 7).

Finally, the calculations presented in this paper are based on the assumption that subsidence is due to the stretching and subsequent thermal equilibration of the lithosphere, and that the stretching homogeneously attenuates the existing heat-producing layer. In reality many intracratonic basins show evidence for subsidence that cannot be ascribed entirely to the effects of rifting (e.g. Hand and Sandiford, 1999). Where subsidence is not due to prior stretching, but factors such as dynamic loads from beneath the lithosphere, the extent of weakening accompanying basin formation may be significantly greater than estimated here because, in these cases, basin formation will not be accompanied by a reduction in the heat production contributed by the pre-existing crust.

Acknowledgements

Richard Hillis and Martin Hand are thanked for many interesting discussions on basin tectonics, which provided an important stimulus for the development of the ideas expressed herein. Teresa Jordan, Jan-Diederik van Wees and an anonymous reviewer are thanked for their careful reviews of the manuscript.

References

Brace, W.F., Kohlstedt, D.L., 1980. Limits on lithospheric strength imposed by laboratory experiments. J. Geophys. Res. 85, 6248–6252.

Buchanan, J.G., Buchanan, P.G., 1995. Basin inversion. Geol. Soc. Spec. Publ. 88, 596 pp.

Cooper, M.A., Williams, G.D., 1989. Inversion tectonics. Geol. Soc. Spec. Publ. 44, 375 pp.

England, P.C., 1983. Constraints on the extension of the continental lithosphere. J. Geophys. Res. 88, 1145–1152.

England, P.C., 1987. Diffuse continental deformation: length scales, rates and metamorphic evolution. Philos. Trans. R. Soc. London A 321, 3–22.

Hand, M., Sandiford, M., 1999. Observations on the role of sediment blanketing in localising intraplate deformation in central Australia during the Alice Springs orogeny. Tectonophysics 305 (this volume).

Hillis, R.R., 1995. Regional Tertiary exhumation in and around the United Kingdom. Geol. Soc. Spec. Publ. 88, 167–190.

Kohlstedt, D.L., Evans, B., Mackwell, S.J., 1995. Strength of the lithosphere: constraints imposed by laboratory experiments. J. Geophys. Res. 100, 17587–17602.

Lachenbruch, A.H., 1968. Preliminary geothermal model of the Sierra Nevada. J. Geophys. Res. 73, 6977–6989.

Liu, L., Zoback, M., 1997. Lithospheric strength and intraplate seismicity in the New Madrid seismic zone. Tectonics 16, 585–595.

Lowell, J.D., 1995. Mechanics of basin inversion from worldwide examples. Geol. Soc. Spec. Publ. 88, 39–58.

McKenzie, D.P., 1978. Some remarks on the development of sedimentary basins. Earth Planet. Sci. Lett. 40, 25–32.

Molnar, P., 1989. Brace–Goetze strength profiles, the partitioning of strike-slip and thrust faulting at zones of oblique convergence and the stress–heat flow paradox of the San Andreas Fault. In: Evans, B., Wong, T.-F. (Eds.), Fault Mechanics and Transport Properties of Rocks. Academic Press, London, pp. 435–460.

Neil, E.A., Houseman, G., 1997. Geodynamics of the Tarim Basin and the Tian Shan in central Asia. Tectonics 16, 571–584.

Ord, A., Hobbs, B., 1989. The strength of the continental crust. Tectonophysics 158, 269–289.

Sibson, R.H., 1995. Selective fault reactivation during basin inversion: potential for fluid redistribution through fault-valve action. Geol. Soc. Spec. Publ. 88, 3–20.

Sonder, L., England, P., 1986. Vertical averages of rheology of the continental lithosphere; relation to thin sheet parameters. Earth Planet. Sci. Lett. 77, 81–90.

van Wees, J.D., Beekman, F., 1999. Lithosphere rheology during intraplate basin extension and inversion. Tectonophysics (in prep.).

van Wees, J.D., Stephenson, R., 1995. Quantitative modelling of basin and rheological evolution of the Iberian Basin (Central Spain): implications for lithospheric dynamics of intraplate extension and inversion. Tectonophysics 252, 163–178.

Ziegler, P.A., Cloetingh, S., van Wees, J.D., 1995. Dynamics of intraplate compressional deformation: the Alpine foreland and other examples. Tectonophysics 252, 7–59.